

THE SPIRAL MODES OF THE SASI: ANGULAR MOMENTUM REDISTRIBUTION AND ORIGIN OF PULSAR SPINS

J. Guilet^{1,2} and Rodrigo Fern andez^{3,4}

Abstract. The accretion shock formed during the collapse of massive stars is subject to the Standing Accretion Shock Instability (SASI). In three-dimensions, spiral modes of this instability can efficiently redistribute angular momentum and thereby impart a spin to the forming neutron star, even when the progenitor star is non-rotating. Here we present an analytical description of the angular momentum redistribution caused by these spiral modes. Our analysis, valid in the limit of small mode amplitude, shows that the angular momentum separation is driven by the Reynolds stress generated by the spiral mode. Analytic solutions compare favorably with previous three-dimensional hydrodynamic simulations of the SASI in the linear and weakly non-linear phases. Reasonable agreement is also found when extrapolating the solutions into the fully non-linear phase. From this analysis, we derive an approximate expression for the minimum period imparted to the neutron star as a function of the relevant accretion flow parameters at the time of explosion. Implications for the birth spin periods of pulsars are discussed.

Keywords: hydrodynamics, instabilities, shock waves, stars: neutron, stars: rotation, supernovae: general

1 Introduction

Neutron stars are formed during the gravitational collapse of massive stars. This core collapse also powers a supernova explosion that ejects the outer layers of the progenitor. The dynamics of the explosion has important consequences for the properties of the resulting neutron star, such as its final mass, space velocity, spin, and magnetic field (see, e.g., Janka 2012 for a review). In particular, the standing accretion shock instability (SASI; Blondin et al. 2003; Ohnishi et al. 2006; Foglizzo et al. 2007; Scheck et al. 2008) causes shock oscillations that create a global asymmetry of the explosion. The SASI is driven by an unstable cycle between the shock and the proto-neutron star surface involving advected and acoustic perturbation (Foglizzo et al. 2007; Foglizzo 2009; Guilet & Foglizzo 2012). Blondin & Mezzacappa (2007) showed that SASI spiral modes have the ability to redistribute angular momentum in the postshock region, and suggested that this process could impart enough angular momentum to the neutron star to significantly change its spin. This angular momentum redistribution was later confirmed by numerical simulations (Blondin & Shaw 2007; Fern andez 2010) and in an experimental analog of SASI (Foglizzo et al. 2012). In this proceeding, we present an analytical description of this angular momentum redistribution, which is described in more detail in Guilet & Fern andez (2013). The formalism is presented in Section 2, and compared with 3D numerical simulations in Section 3. Finally, in Section 4 we give an approximate expression for the spin that can be imparted to the neutron star by this process and discuss the consequences for neutron star rotation periods at birth.

2 Formalism

We consider a standing spherical accretion shock around a central protoneutron star of mass M and radius r_* that is subject to a spiral SASI mode around some axis. The upstream accretion flow is non-rotating. We assume

¹ Department of Applied Mathematics and Theoretical Physics, University of Cambridge
Centre for Mathematical Sciences, Wilberforce Road, Cambridge CB3 0WA, UK

² Max-Planck-Institut fur Astrophysik, Karl-Schwarzschild-Str. 1, D-85748 Garching, Germany

³ Department of Physics, University of California, Berkeley, CA 94720, USA

⁴ Department of Astronomy & Theoretical Astrophysics Center, University of California, Berkeley, CA 94720, USA

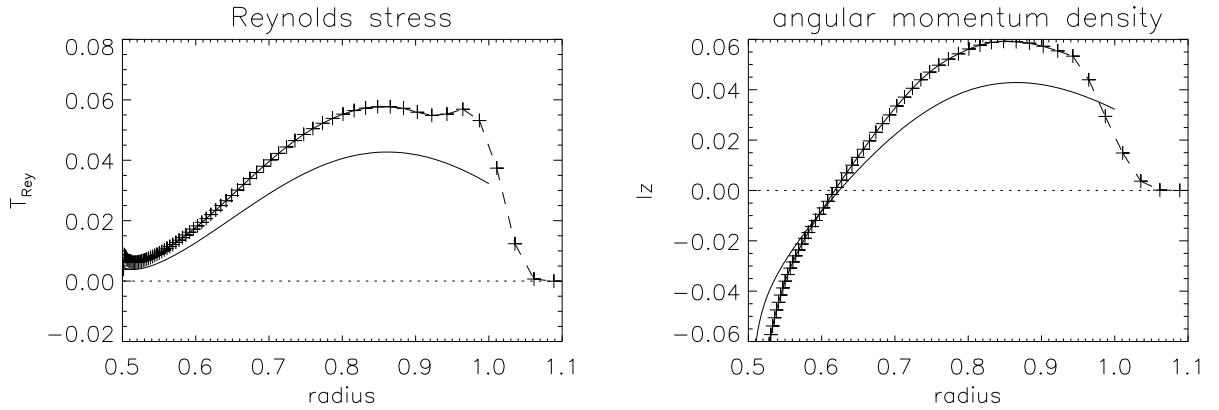


Fig. 1. Radial profiles of the surface-integrated Reynolds stress (left) and angular momentum density (right) resulting from an $l = 1$ spiral mode. The radius is normalized by the shock radius, the Reynolds stress by $M\dot{r}_{\text{sh0}}|v_{\text{sh0}}|$, and the angular momentum density by $M\dot{r}_{\text{sh0}}$. The dashed lines with + signs show values from model R5_L11_HR of Fernández (2010) at $t = 30$, while the full lines show the semi-analytical predictions. See Guilet & Fernández (2013) for details.

that the flow can be described as a stationary background with superimposed small amplitude perturbations:

$$\rho(r, \theta, \phi, t) = \rho_0(r) + \delta\rho(r, \theta, \phi, t) + \delta^2\rho(r, \theta, \phi, t) + \dots \quad (2.1)$$

$$v_r = v_0 + \delta v_r + \delta^2 v_r + \dots \quad (2.2)$$

$$v_\phi = \delta v_\phi + \delta^2 v_\phi + \dots \quad (2.3)$$

where δ and δ^2 denote first- and second order Eulerian perturbations, respectively, with $\delta \gg \delta^2$. We retain perturbations up to second order because this is the first non-zero contribution to the surface integrated angular momentum l_z . The evolution of the first order perturbations can be computed with a linear analysis as in Foglizzo et al. (2007).

Using this expansion, the angular momentum conservation can be written as:

$$\partial_t l_z + \partial_r(l_z v_0) = -\partial_r T_{Rey}, \quad (2.4)$$

where $l_z \equiv \iint r \sin\theta \rho v_\phi d^2s$ is the angular momentum density integrated over a spherical shell, and $T_{Rey} \equiv \iint \rho_0 \delta v_r \delta v_\phi r \sin\theta d^2s$ is the surface integrated Reynolds stress, describing the angular momentum flux driven by the non-axisymmetric perturbations of the spiral mode. The Reynolds stress can be computed using the linear eigenmodes and Equation (2.4) can then be solved to obtain the angular momentum density driven by a SASI spiral mode:

$$l_z = -\frac{T_{Rey}}{v_0} + \frac{e^{-2\omega_i \tau_{\text{adv}}}}{v_0} \int_{r_{\text{sh}}}^r \frac{2\omega_i e^{2\omega_i \tau_{\text{adv}}}}{v_0} T_{Rey} dr, \quad (2.5)$$

where ω_i is the growth rate of the spiral mode, and τ_{adv} is the advection time from the shock to the radius r considered.

3 Comparison with numerical simulations

We now compare these analytical predictions with the 3D numerical simulations of Fernández (2010). Figure 1 shows the radial profile of the surface integrated Reynolds stress and angular momentum density in the linear phase of their model R5_L11_HR dominated by a spiral mode with spherical harmonics $\{l, m\} = \{1, 1\}$. The analytically predicted shapes of the Reynolds stress and angular momentum profiles agree very well with the numerical simulations, while the magnitude match within 30% which is the expected accuracy given the numerical resolution. The Reynolds stress has the same sign as m , thus transporting angular momentum outward. On the other hand, the angular momentum density changes sign at an intermediate radius: angular momentum redistribution caused by the Reynolds stress creates a region of positive angular momentum below the shock, and a region of negative angular momentum above the PNS surface.

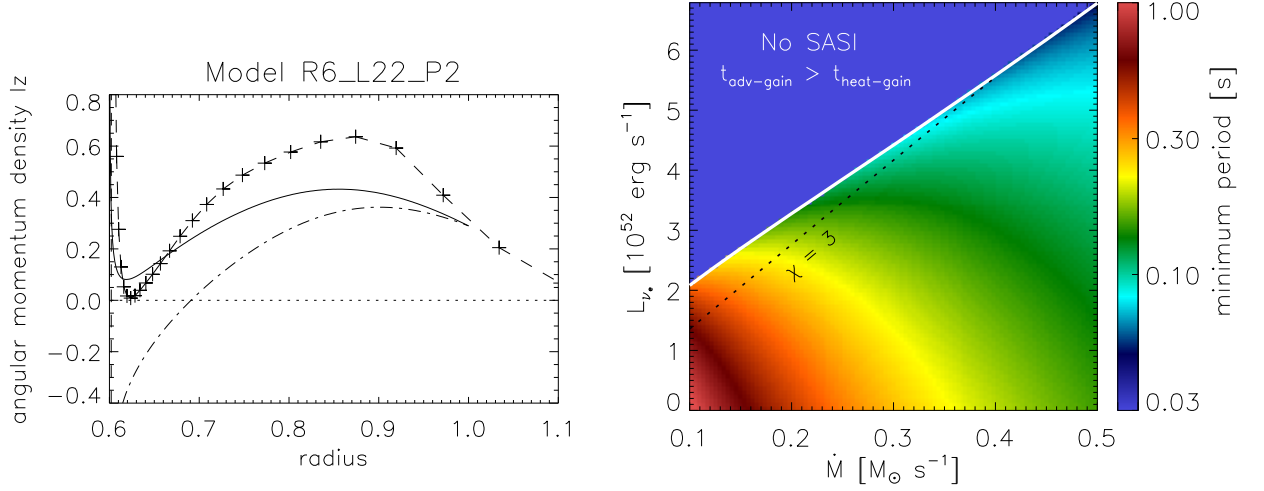


Fig. 2. Left: Time-averaged profile of surface integrated angular momentum density in the non-linear phase of model R6.L22.P2 dominated by an $\{l, m\} = \{2, 2\}$ spiral mode. Simulation results are shown with + signs and a dashed line, while the analytical prediction extrapolated to the saturated phase is shown with a full black line. For comparison, we also show the predicted angular momentum density in the case of a growing mode (from eq. 2.5, dot-dashed black line). **Right:** Minimum neutron star rotation period that can be generated via a spiral SASI mode, as inferred from equation (4.1). The input parameters (shock radius, shock compression ratio, SASI period, and postshock velocity) are computed from the steady-state solutions of Fernández (2012), which employ a realistic equation of state. The region marked ‘No SASI’ is such that the runaway condition in spherical symmetry (Janka & Keil 1998) is met, thus the SASI does not have time to develop before explosion. The dashed line shows the threshold $\chi = 3$, below which the SASI is expected to dominate the dynamics (Foglizzo et al. 2006). See Guilet & Fernández (2013) for details.

In the non-linear phase of SASI activity, our approximations are not valid anymore, in particular because the spiral mode stops growing. This can be approximately taken into account to extrapolate our results to the non-linear phase by setting the growth rate to zero, in which case Equation (2.5) becomes: $l_z = -\frac{T_{Regy}}{v_0}$. The left panel of Figure 2 shows that this prediction is in acceptable agreement with the time-averaged angular momentum profile of model R6.L22.P2 of Fernández (2010). In contrast to the linear phase, the angular momentum density is positive over most of the domain because matter with the opposite sign of angular momentum has had time to accrete onto the protoneutron star.

4 Approximate expression for the neutron star spin

When the explosion occurs, a net spin can be imparted to the forming neutron star if the matter below the shock with an angular momentum of a given sign is ejected while the matter with the opposite sign of angular momentum is accreted onto the protoneutron star (Blondin & Mezzacappa 2007). A simple approximate expression for the total angular momentum redistributed by a SASI spiral mode can be obtained by approximating the radial profile of angular momentum density by a flat profile. This analytical estimate is found to agree with the numerical simulations of Fernández (2010) within a few tens of percents. Assuming a moment of inertia of the neutron star of $I = I_{45} \times 10^{45} \text{ g.cm}^2$, we can then estimate the minimum period of uniform rotation of the neutron star in the optimistic scenario where all this angular momentum is ejected:

$$P \simeq 290 I_{45} \left(\frac{10}{\kappa} \right) \left(\frac{P_{sasi}}{50 \text{ ms}} \right) \left(\frac{120 \text{ km}}{r_{sh} - r_*} \right) \left(\frac{v_{sh}}{3000 \text{ km.s}^{-1}} \right) \left(\frac{0.3 M_{\odot} \text{.s}^{-1}}{\dot{M}} \right) \left(\frac{150 \text{ km}}{r_{sh}} \right)^2 \left(\frac{r_{sh}}{3\Delta r} \right)^2 \text{ ms.} \quad (4.1)$$

where κ is the compression ratio of the shock, P_{sasi} the oscillation period of the SASI spiral mode, r_{sh} and r_* the radii of the shock and protoneutron star respectively, \dot{M} the mass accretion rate, and Δr the amplitude of the shock deformation caused by the spiral mode. Note the dependence on the square of the amplitude and the shock radius.

The right panel of Figure 2 shows the result of evaluating equation (4.1) with parameters from the steady-state accretion shock models of Fernández (2012). The minimum period is computed as a function of the mass

accretion rate and electron neutrino luminosity, assuming a spiral mode amplitude $\Delta r = 0.3r_{\text{sh}}$. This figure shows that shorter periods are obtained with larger neutrino luminosities – which yield larger shock radii – and larger accretion rates. The normalization indicates that massive progenitors with large accretion rates, where strong SASI activity is expected (Müller et al. 2012; Hanke et al. 2013; Ott et al. 2013), can lead to periods ~ 100 ms or less. In contrast, progenitors that have a lower accretion rate and which may be expected to suppress SASI activity (e.g., Müller et al. 2012; Takiwaki et al. 2012; Murphy et al. 2013; Dolence et al. 2013; Couch 2013), would otherwise acquire very moderate amounts of angular momentum if the SASI were present, with minimum periods in the range 0.3 – 1 s. Note that the latter value is comparable to the spin periods obtained by Wongwathanarat et al. (2010, 2013).

From an observational point of view, the spin of neutron stars at birth is still poorly constrained. The difficulty comes from the fact that the observed period of pulsars is very different from their initial period because of spin down, and that the true age of most pulsars is unknown. Population synthesis studies nevertheless suggest that a distribution of initial spin peaking around 300 ms is consistent with observations (e.g., Faucher-Giguère & Kaspi 2006). The age of some pulsars can be estimated when they are associated with a supernova remnant, which then allows to constrain their initial spin period. Despite poor statistics and sometimes large uncertainties, these observations suggest that a significant fraction of neutron stars have initial periods longer than 100 ms (e.g. Popov & Turolla 2012 and references therein). The range of pulsar spin periods we obtain is therefore of the same order of magnitude as that inferred from the observations, and we conclude that angular momentum redistribution by a SASI spiral mode can be relevant to explain these observations.

5 Conclusions

We have developed an analytical description of the angular momentum redistribution driven by SASI spiral modes, which compares favorably with the results of the 3D numerical simulations of Fernández (2010). Angular momentum redistribution is due to the Reynolds stress of the SASI mode, which causes angular momentum with the same rotation direction as the spiral mode to accumulate below the shock, while angular momentum with the opposite sign is accreted onto the proto-neutron star.

We derived an approximate analytical expression for the maximum angular momentum that can be imparted to the neutron star if all the SASI active region is ejected during the explosion. The expected minimum neutron star spin periods in uniform rotation are comparable with values estimated by observations of pulsars associated with supernova remnants and by population synthesis studies for the bulk of the pulsar population. Our analysis further suggests that the angular momentum of the nascent neutron star should be positively correlated with the mass accretion rate at the time of explosion if progenitors are slowly rotating. As a consequence, neutron stars born from progenitors with a shallow density profile – for which the SASI should dominate the explosion dynamics (e.g., Müller et al. 2012; Hanke et al. 2013; Iwakami et al. 2013) – should rotate faster on average than those arising from stars with steeper profiles, which are generally less massive.

We emphasize that the analytical formula for the angular momentum redistributed by a spiral mode depends strongly on the amplitude of the spiral mode, which was taken as an input from the simulations. A semi-analytical description of the saturation of SASI as obtained by Guilet et al. (2010) could then be combined with our treatment to obtain a fully predictive analytical description of the angular momentum redistribution.

Note that the above prediction is contingent on a very optimistic scenario in which the mass cut at explosion coincides with the surface where the angular momentum changes sign. Prolonged SASI activity up to the point of explosion, as seen in the 2D models of Müller et al. (2012), is essential for this spin-up mechanism to work. Furthermore, our analysis applies if the initial rotation of the progenitor is negligibly slow. More generally, the initial spin of neutron stars is likely to result from a combination of angular momentum initially present in the progenitor and that redistributed by the SASI. Further studies using a rotating progenitor will be needed to clarify the consequences on the dynamics and on the spin of neutron stars.

Finally, we note that the present study neglects the effects of magnetic fields, which can transport angular momentum via the Maxwell stress. The influence of a magnetic field on the linear growth of SASI has been studied in a planar toy model by Guilet & Foglizzo (2010). One possible extension of the present study is including magnetic effects in the angular momentum redistribution in spherical or even cylindrical coordinates. Guilet et al. (2011) have shown that Alfvén waves can be amplified in the vicinity of an Alfvén surface, where the advection velocity equals the Alfvén speed. This phenomenon may also have interesting consequences on the angular momentum redistribution.

We thank Henrik Latter, Thierry Foglizzo and Benjamin Favier for helpful discussions. JG acknowledges support from the STFC and from the Max-Planck-Princeton Center for Plasma Physics. RF acknowledges support from the University of California Office of the President, and from NSF grants AST-0807444 and AST-1206097.

References

- Blondin, J. M. & Mezzacappa, A. 2007, *Nature*, 445, 58
- Blondin, J. M., Mezzacappa, A., & DeMarino, C. 2003, *ApJ*, 584, 971
- Blondin, J. M. & Shaw, S. 2007, *ApJ*, 656, 366
- Couch, S. M. 2013, *ApJ*, 775, 35
- Dolence, J. C., Burrows, A., Murphy, J. W., & Nordhaus, J. 2013, *ApJ*, 765, 110
- Faucher-Giguère, C.-A. & Kaspi, V. M. 2006, *ApJ*, 643, 332
- Fernández, R. 2010, *ApJ*, 725, 1563
- Fernández, R. 2012, *ApJ*, 749, 142
- Foglizzo, T. 2009, *ApJ*, 694, 820
- Foglizzo, T., Galletti, P., Scheck, L., & Janka, H.-T. 2007, *ApJ*, 654, 1006
- Foglizzo, T., Masset, F., Guilet, J., & Durand, G. 2012, *PRL*, 108, 051103
- Foglizzo, T., Scheck, L., & Janka, H.-T. 2006, *ApJ*, 652, 1436
- Guilet, J. & Fernández, R. 2013, *ArXiv e-prints*
- Guilet, J. & Foglizzo, T. 2010, *ApJ*, 711, 99
- Guilet, J. & Foglizzo, T. 2012, *MNRAS*, 421, 546
- Guilet, J., Foglizzo, T., & Fromang, S. 2011, *ApJ*, 729, 71
- Guilet, J., Sato, J., & Foglizzo, T. 2010, *ApJ*, 713, 1350
- Hanke, F., Müller, B., Wongwathanarat, A., Marek, A., & Janka, H.-T. 2013, *ApJ*, 770, 66
- Iwakami, W., Nagakura, H., & Yamada, S. 2013, *ApJ*, submitted, arXiv:1308.0829
- Janka, H.-T. 2012, *Ann. Rev. Nuc. Part. Sci.*, 62, 407
- Janka, H.-T. & Keil, W. 1998, in *Supernovae and cosmology*, ed. L. Labhardt, B. Binggeli, & R. Buser, 7
- Müller, B., Janka, H.-T., & Heger, A. 2012, *ArXiv e-prints*
- Murphy, J. W., Dolence, J. C., & Burrows, A. 2013, *ApJ*, 771, 52
- Ohnishi, N., Kotake, K., & Yamada, S. 2006, *ApJ*, 641, 1018
- Ott, C. D., Abdikamalov, E., Mösta, P., et al. 2013, *ApJ*, 768, 115
- Popov, S. B. & Turolla, R. 2012, *Ap&SS*, 341, 457
- Scheck, L., Janka, H.-T., Foglizzo, T., & Kifonidis, K. 2008, *A&A*, 477, 931
- Takiwaki, T., Kotake, K., & Suwa, Y. 2012, *ApJ*, 749, 98
- Wongwathanarat, A., Janka, H.-T., & Müller, E. 2010, *ApJ*, 725, L106
- Wongwathanarat, A., Janka, H.-T., & Müller, E. 2013, *A&A*, 552, A126